J. Astron. Space Sci. 17(1), 1–10 (2000)

METALLICITIES OF GLOBULAR CLUSTERS M3 AND M5 FROM *VI* CCD PHOTOMETRY

Young-Jong Sohn[1] and Hyun-chul Lee[1,2]

[1] Center for Space Astrophysics, Yonsei University, Seoul, 120-749, Korea

[2] Department of Astronomy, Yonsei University, Seoul, 120-749, Korea

email : sohnyj@csa.yonsei.ac.kr, hclee@csa.yonsei.ac.kr

(Received March 21, 2000; Accepted May 15, 2000)

ABSTRACT

To derive the metallicities of M3 and M5, we used the shape of red giant branch, horizontal branch magnitude, and red giant branch bump on the $(V-I)-V$ color magnitude diagrams. [Fe/H] values ranging $-1.46 \sim -1.69$ for M3, and $-1.00 \sim -1.49$ for M5 are estimated. These values are in good agreements with the previously determined ones. This result leads the morphologies of red giant and horizontal branches on the $(V-I)-V$ color magnitude diagrams can be good indirect metallicity indicators of galactic globular clusters.

1. INTRODUCTION

Metal contents of galactic globular clusters, measured by the [Fe/H] ratios, provide strong constraints on models of galactic formation. The most widely used metallicity scale for globular clusters has been the one obtained by Zinn & West (1984) from a calibration of integrated parameter Q_{39}. Recently, Carretta & Gratton (1997) used high dispersion, high S/N spectra of more than 160 red giants in 24 clusters to derive new metallicity scale based on direct abundance analysis, coupled with the Kurucz (1992) model atmospheres. They demonstrated that the Zinn & West (1984)'s scale is clearly non-linear in comparison to their improved scale.

Abundance analysis using the high resolution spectra is the best way to get a quantitatively accurate estimate of the metal abundance of any star in a globular cluster. However, high resolution spectroscopy of stars in a globular cluster is very time consuming, and can be obtained only for the brightest giants because of their large distances. Therefore several indirect metallicity indicators, which require a relatively accurate calibration to provide the true content in [Fe/H], have been devised. For example, metallicity indicators can be derived from the red-giant-branch (RGB) and the horizontal-branch (HB) morphologies of globular clusters with good Color-Magnitude Diagrams (CMDs) of the brightest evolutionary phases. The position and morphology of the RGB in CMDs are theoretically well tied to the metal contents of the stars in a cluster: the higher the metal content, the cooler the effective temperature and the redder the RGB stars. Sarajedini (1994) devised the simultaneous metallicity and reddening (SMR) method for globular clusters in the $(V-I)-V$ CMD plane, using the $(V-I)_o$ value of RGB measured at the level of HB, and the difference in V between the HB and RGB at $(V-I)_o = 1.2$. His calibration was based on the Zinn & West (1984)'s scale and high precision CCD photometry obtained by Da Costa & Armandroff (1990). Recently,

Carretta & Bragaglia (1998) gave new accurate relations to employ the method by Sarajedini (1994), tied to the Carretta & Gratton (1997) abundance scale.

In this study, we applied Sarajedini (1994)'s SMR method on the $(V-I)-V$ CMDs for M3 and M5 in order to derive their metallicities and reddenings and other physical parameters such as the HB magnitudes. The relation between metallicity and RGB bump luminosity is also used to derive metallicities. The observation, data reduction, and standardization procedure are described in Sec. 2. In Sec. 3, we show the $(V-I)-V$ CMDs of M3 and M5, and derive the mean V magnitudes of HB for each cluster. In Sec. 4, we determine the metallicities of each cluster and compare them with the previously determined ones, and summarize our results.

2. OBSERVATION, DATA REDUCTION, AND STANDARDIZATION

VI images of globular clusters M3 and M5 were obtained over the night in UT 1999 March 23 using the 1.8m telescope at BOAO. The detector was SITe CCD chip of 2048 × 2048 format. At the f/8 Cassegrain focus, the image scale is 0.34 arcsec pixel^{-1}, which gives the sky coverage of 11.8 × 11.8 arcmin^2. A single exposure centered on the cluster center was taken in each V and I filter with the exposure times of 180 and 60 seconds for M3, and 60 and 20 seconds for M5, respectively. The night of the run was fully photometric, and the seeing measured from the reduced images is $\sim 1.0-1.1$ arcsec FWHM.

The data reduction followed standard processing lines. The bias level and pattern were removed by subtracting both a fit to the overscan region and a master zero-level frame. The results were then divided by twilight flats to remove additional pixel-to-pixel variations through the frame.

Observations were also made of a number of standard stars on the Landolt (1992) fields, including SA 98, Rubin 149, and Rubin 152. The observations were made over a range of airmass from 1.25 to 1.28, and the stars range in $V-I$ color from $-0.2 \sim 2.1$ mag. Multiple aperture photometry was performed using the DAOPHOT II (Stetson 1987) PHOT task on each of the standard frames. This result was then used as input to the program DAOGROW (Stetson 1990), which makes a growth-curve analysis to derive total magnitudes for each star. This magnitude was corrected for the exposure time of the frame. Extinction coefficients, which were estimated from the data of time-series observations of NGC 5024, are $k_V = 0.204$ and $k_I = 0.066$, respectively. The photometric transformations were assumed to have the following forms:

$$\begin{aligned} V - v_o &= \epsilon(v-i)_o + \zeta_V \\ (V-I) &= \mu(v-i)_o + \zeta_{V-I}. \end{aligned} \tag{1}$$

Our transformation coefficients are $\epsilon = -0.044 \pm 0.014, \zeta_V = -2.528 \pm 0.011, \mu = +0.962 \pm 0.022$, and $\zeta_{V-I} = +0.244 \pm 0.017$. The rms differences between our observations and the standard system are 0.019 and 0.030 mag in V and $V-I$, respectively. Figure 1 shows the residuals of $(V-I)$ and V in the sense of Landolt (1992) minus our work for the selected standard stars.

3. COLOR-MAGNITUDE DIAGRAM AND THE HORIZONTAL BRANCH

The V and I magnitudes of individual stars in M3 and M5 were measured with the PSF-fitting photometry package DAOPHOTII/ALLSTAR (Stetson 1987, Stetson & Harris 1988). To calculate the point spread functions, we used $\sim 90-100$ isolated bright stars located at radii larger than 500 pixels from the cluster center, within which stars can be affected by the crowding effect. An iterative method has been applied to remove neighboring stars of selected PSF stars, so that we were

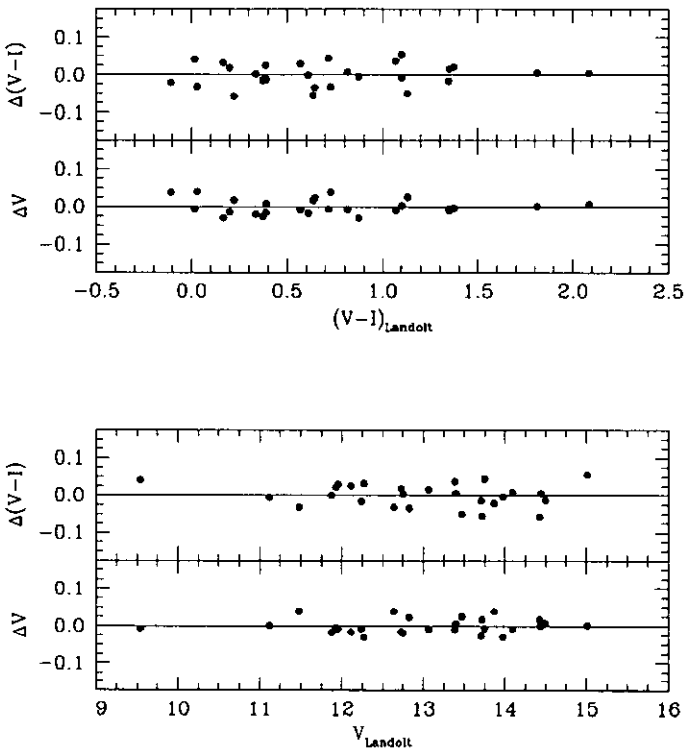

Figure 1. Residuals of $(V - I)$ and V in the sense of Landolt (1992) minus our work for the selected standard stars.

able to achieve appropriate PSFs for each frame. After the first ALLSTAR pass, we undertook two additional passes to find more faint stars on the subtracted frames. Using the growth-curve method DAOGROW, the mean difference between the PSF-based magnitude and the total magnitude of selected PSF stars, was calculated in each frame. This aperture correction was applied to PSF-based magnitudes for every stars in the frame. Airmass corrections, and finally photometric transformations were then applied to derive the standard magnitudes of stars in both of cluster frames.

To construct the CMD, we derived the positional transformation solutions for the VI pairs of each cluster using DAOMATCH and DAOMASTER (Stetson 1992). The size of match-up radius on the DAOMASTER procedure has been reduced until the rms residuals of x- and y- positions for each frame were less than 0.1 pixels. Finally, total 19,759 and 19,394 stars were detected in both V and I images of M3 and M5, respectively. Figure 2 shows $(V - I) - V$ CMDs of stars in M3 and M5 having $\chi \leq 1.2$, which quantifies how well the empirically derived PSF for a frame matched a star's actual profile. The CMDs of M3 and M5 reveal HBs that are populated on both sides of the RR Lyrae instability strip. This fact is not surprising given the large number of RR Lyrae variables in each cluster. Indeed, Sawyer-Hogg (1973) listed 225 and 103 variable stars in M3 and M5, and Clement (1999) has added 15 and 26 more variable stars in each cluster. Fiducial sequences of Johnson & Bolte (1998) are plotted on Figure 2 as solid lines, showing good agreements with our results.

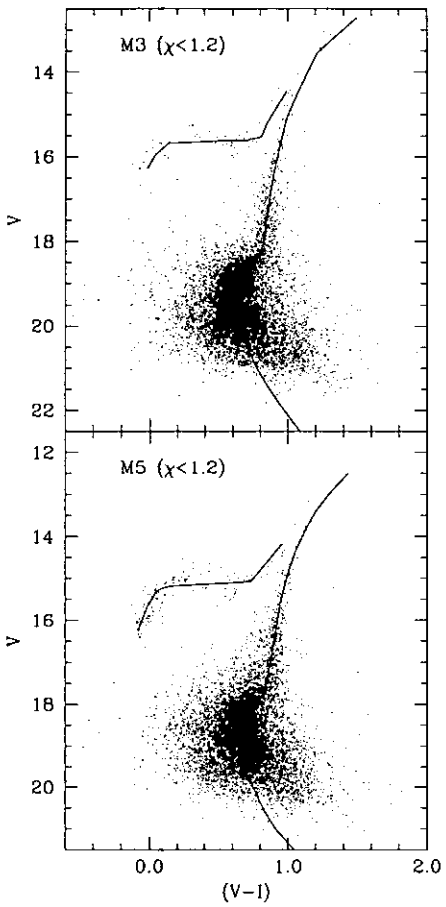

Figure 2. $(V-I)-V$ CMDs of stars in M3 and M5 having $\chi < 1.2$. Fiducial sequences of Johnson & Bolte (1998) are plotted as solid lines.

Figures 3 and 4 show HB stars of M3 and M5 having χ less than 1.2 and radius larger than core radius of each cluster. It is apparent that there are many sub-luminous stars on the red HBs and several more luminous stars on the red end of blue HBs of both clusters (*top panels* of Figures 3 and 4). Cross identification of positional data of these stars and variable stars of M3 and M5 listed in in Sawyer-Hogg (1973) and Clement (1999) reveals that most of these stars are RR Lyrae variable stars in each cluster. The *middle panels* of Figures 3 and 4 show the HB of M3 and M5 with the identified variable stars plotted as open circles. Finally, the mean magnitudes of the HBs of each cluster are estimated by computing the mean V of the non-variable stars in the two dashed boxes on the *lower panels* of Figures 3 and 4. These yield V(HB)= 15.58 ± 0.08 and 15.05 ± 0.12 for M3 and M5, respectively. These are in good agreement with V(HB)= 15.63 and 15.05 derived by Chaboyer et al. (1998). The quoted errors are composed of standard errors of the means and estimated uncertainty in the photometric zero point of ±0.019 mag (see Sec. 2).

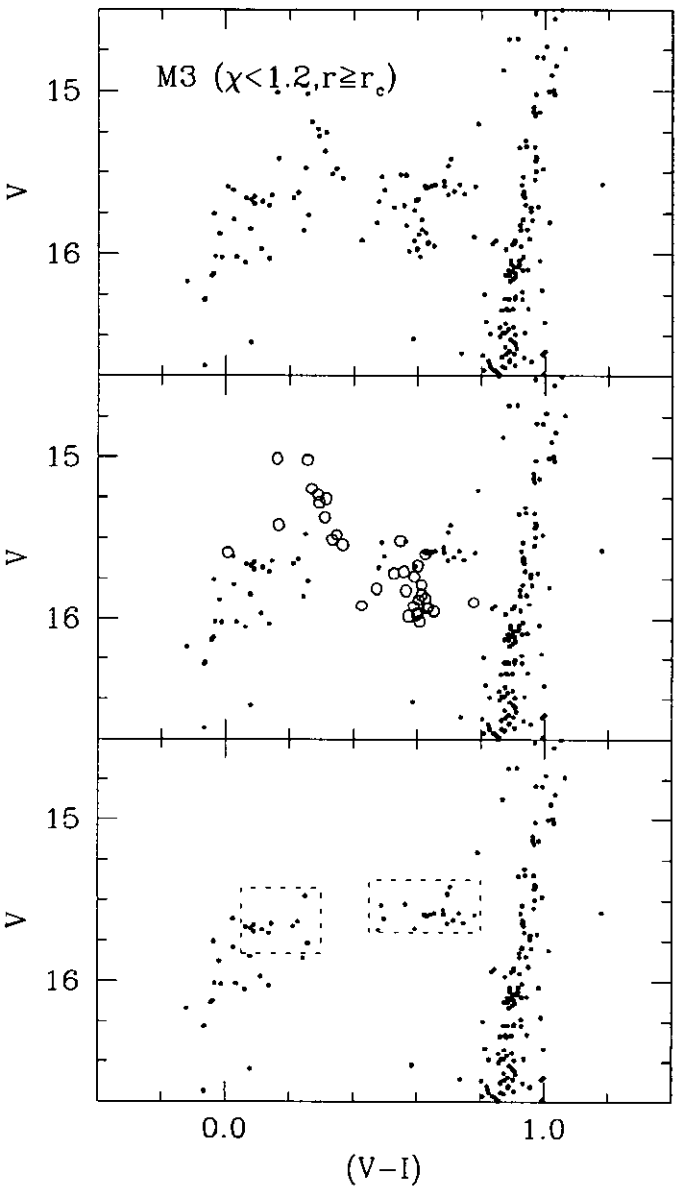

Figure 3. (Top) HB stars of M3 having $\chi < 1.2$ and radius larger than core radius. (Middle) HB stars of M3 with the previously known RR Lyrae variable stars plotted as open circles. (Bottom) HB stars of M3 with variable stars removed. Dashed boxes are used to determine the mean magnitude of HB.

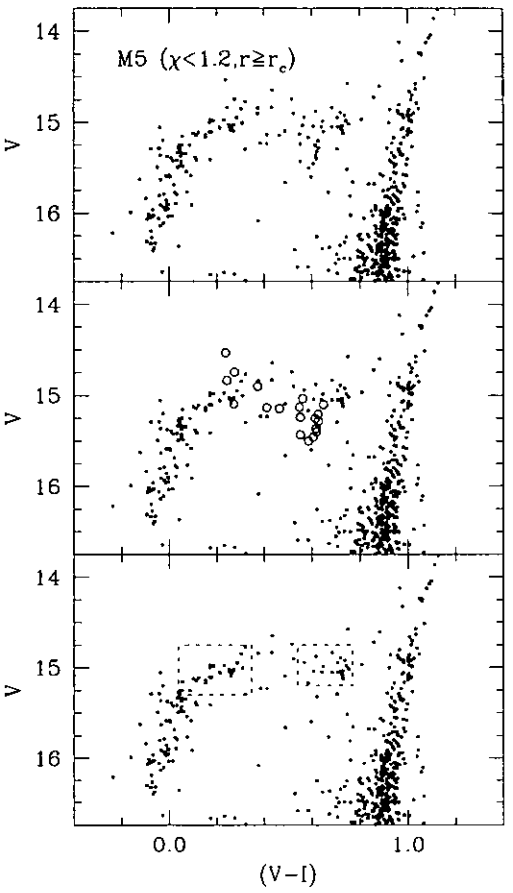

Figure 4. HB stars of M5. Same as Figure 3.

4. METALLICITY

In most cases deriving basic parameters such as reddening and metallicity from the CMDs of globular clusters, one of these quantities is adopted depending on which is known to higher precision. The other parameter is then derived using a calibration between RGB position and metal abundance. Sarajedini (1994) called the weakness of this method in question and suggested a technique by which the metal abundance and reddening of a globular cluster can be derived simultaneously using the shape of the RGB and observed value of the HB magnitude [i.e., V(HB)] and the $V-I$ color of the RGB at the level of the HB [i.e., $(V-I)_g$]. Here, we apply this method to derive the metallicity and reddening of M3 and M5 with the V(HB)s derived in Sec. 3.

RGB shapes on the CMDs of each cluster have been determined using a quadratic relation of the form $V-I = a_0 + a_1 V + a_2 V^2$. The appropriate coefficients have been derived from fitting the relation on the RGB area plotted as dashed lines in Figure 5. RGB regions were defined from the eye-fitting of RGB fiducial line and its widths on $V-I$ color. We listed the derived coefficients in

Table 1. Quadratic coefficients of RGB shapes of M3 and M5.

cluster	a_0	a_1	a_2
M3	6.546669	-0.633188	0.017550
M5	6.503987	-0.635690	0.017896

Table 2. Globular cluster parameters.

cluster	V(HB)	$(V-I)_g$	$\Delta V_{1.2}$	E$(V-I)$	[Fe/H]$_{S94}$	[Fe/H]$^1_{CB98}$	[Fe/H]$^2_{CB98}$	[Fe/H]$_{SF95}$
M3	15.58	0.942	2.10	0.01	-1.69	-1.52	-1.46	-1.55
	±0.08	±0.007	±0.08		±0.08			
M5	15.05	0.990	1.66	0.02	-1.29	-1.10	-1.00	-1.49
	±0.12	±0.011	±0.12		±0.12			

[Fe/H]$_{S94}$: based on Sarajedini (1994)
[Fe/H]$^1_{CB98}$: based on the relation between [Fe/H] and $\Delta V_{1.2}$ of Carretta & Bragaglia (1998)
[Fe/H]$^2_{CB98}$: based on the relation between [Fe/H] and $(V-I)_{o.g}$ of Carretta & Bragaglia (1998)
[Fe/H]$_{SF95}$: based on Sarajedini & Forrester (1995)

Table 1, and plotted quadratic formulae for RGB stars of M3 and M5 as solid line on Figure 5. The horizontal line indicates the level of V(HB). We converted coefficients b_0, b_1, and b_2 of the Eq.(6) and Eq.(7) of Sarajedini (1994) to the forms of a_0, a_1, a_2, and V(HB) as follows.

$$\begin{aligned} b_0 &= -1.2 + a_0 + a_1 V(HB) + a_2 V^2(HB) \\ b_1 &= -a_1 - 2a_2 V(HB) \\ b_2 &= a_2 \end{aligned} \tag{2}$$

Applying these relations to the Eq.(6) and Eq.(7) of Sarajedini (1994), we could estimate the reddening E$(V-I)$ and metal abundance [Fe/H] of each cluster simultaneously. We have used $\Delta V_{1.2}$ and $(V-I)_g$ as input parameters. Here, $\Delta V_{1.2}$ is the difference in V between the HB and the RGB at $V-I=1.2$, and $(V-I)_g$ is the $V-I$ color of the RGB measured at the level of HB. At V(HB)$= 15.58 \pm 0.08$ of M3 and 15.05 ± 0.12 of M5 (see Sec. 3), quadratic fits to the RGB stars give $(V-I)_g = 0.942 \pm 0.007$ for M3, 0.990 ± 0.011 for M5, respectively. We obtained metal abundances of [Fe/H]$= -1.69 \pm 0.08$ and -1.29 ± 0.12, and reddenings E$(V-I) = 0.01$ and 0.02 for M3 and M5, respectively. Note that Sarajedini (1994)'s calibration was based on Zinn & West (1984) metallicity scale. Therefore we also applied Carretta & Bragaglia (1998)'s new relations, tied to the Carretta & Gratton (1997) abundance scale, to estimate metallicities. From the relation between [Fe/H] and $\Delta V_{1.2}$, we derived [Fe/H]$= -1.52$ and -1.10 for M3 and M5. Also, metallicities are derived to be [Fe/H]$= -1.46$ and -1.00 for M3 and M5 from the relation between [Fe/H] and $(V-I)_{o.g}$.

The luminosity function (LF) of the RGB in some globular clusters shows a clump of stars, which is called as RGB bump, an evolutionary pause on the first-ascent RGB (e.g., Iben 1968). The luminosity of the RGB bump is primarily dependent on the cluster metal abundance. Fusi Pecci et al. (1990) have shown that it is best to express the apparent magnitude of the bump relative to that of the HB [i.e., $\Delta V^{HB}_{Bump} = V$(Bump)$-V$(HB)], compiling ΔV^{HB}_{Bump} values of 11 globular clusters. Adding data for 5 additional clusters, Sarajedini & Forrester (1995) derived the relation between metallicity and the RGB bump luminosity, i.e., [Fe/H] $= -1.33 + 1.43 \Delta V^{HB}_{Bump}$. We have also

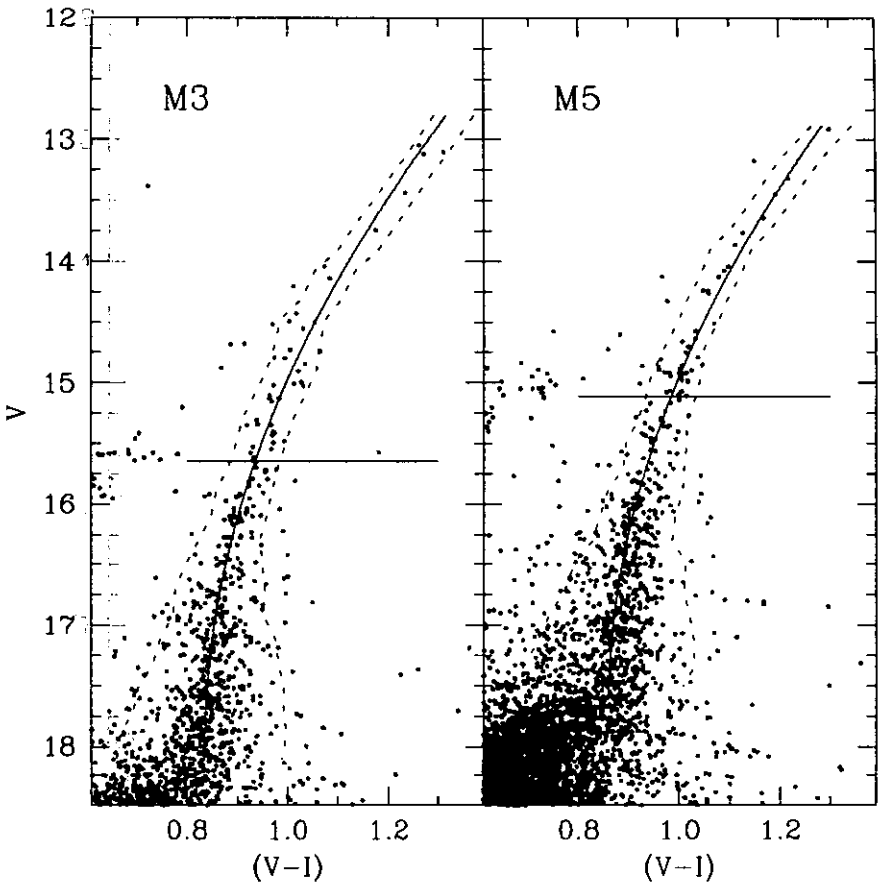

Figure 5. RGB stars of M3 and M5. Quadratic formulae of RGB shapes and the level of V(HB) are also plotted.

used this equation to derive the metal abundance of M3 and M5. We proceed by first determining the magnitude of RGB bump. Since the bump exhibits a break of slope in the cumulative LF, the cumulative LF is known to be a useful tool to detect the RGB bump. In Figure 6, we present the cumulative LFs for M3 and M5 RGB stars located at radius larger than the cluster's core radius with a binning size of 0.05 mag. It is apparent that there is RGB bump at the magnitude of 14.93 ± 0.05 for M5. The RGB bump of M3 is not clearly detected on the cumulative LF. Neverthless, we could adopt $V_{Bump} = 15.43 \pm 0.05$, considering the CMD morphology of M3 on Figure 5. Here, the quoted error is just the binning size of the LF. Using V(HB)s of each cluster in Sec. 3, we obtained $\Delta V^{HB}_{Bump} = -0.15 \pm 0.09$ and -0.12 ± 0.13, which yield [Fe/H] $= -1.55 \pm 0.08$ and -1.49 ± 0.18 for M3 and M5, respectively. Note the field star contamination on RGB stars in this study is almost negligible, since both M3 and M5 lie at a fairly high galactic latitudes ($b = 79^o$ and 47^o for M3 and M5, respectively), and only stars located at radius larger than the cluster's core radius have been used in the LF analysis.

Table 2 lists metallicities and the other parameters derived for M3 and M5 in this paper. [Fe/H]

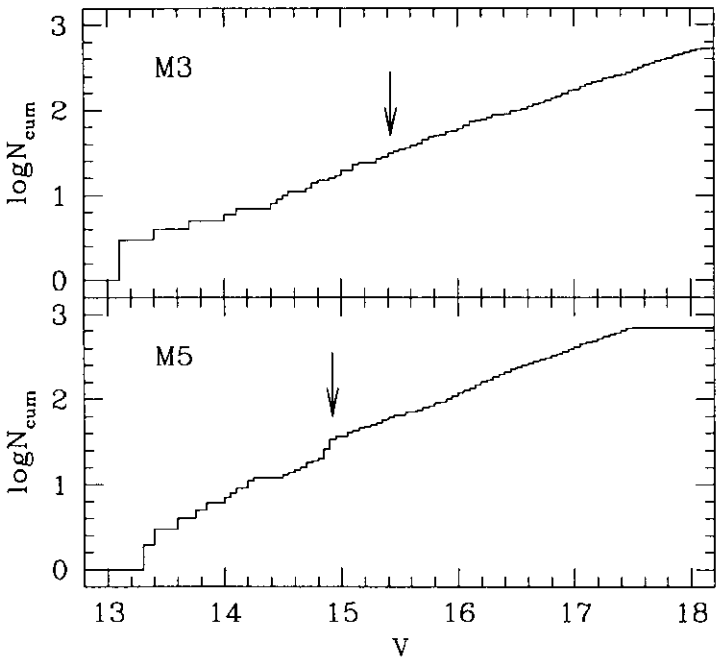

Figure 6. Cumulative luminosity functions of RGB stars in M3 and M5. Arrows indicate the RGB bumps.

values range $-1.46 \sim -1.69$ for M3, and $-1.00 \sim -1.49$ for M5. For M3, Kraft et al. (1992) found [Fe/H]$= -1.47$, based on detailed fine abundance analysis of high resolution spectra of red giants. Their study is, however, not fully consistent on the model atmosphere and empirical solar iron abundance (Rood et al. 1999). Sneden et al. (1992) derived [Fe/H]$= -1.17$ for M5 from the Echelle spectra of 13 giants. They also provide a summary of many of the metallicity determinations for M5 made in the past 20 years, i.e., [Fe/H] values ranging from -1.09 to -1.5. Carretta & Gratton (1997) gave [Fe/H]$=-1.34$ and -1.17 for M3 and M5 respectively, using the Kurucz (1992) grid of model atmospheres for both solar and stellar analysis. Zinn & West (1984) returned [Fe/H]$= -1.66$ and -1.40 for M3 and M5, respectively.

In conclusion, metallicities of M3 and M5 derived in this paper are in good agreements with the previously determined ones. This result leads the morphologies of RGB and HB on the $(V-I)-V$ CMDs can be good indirect metallicity indicators. A large and homogeneous CCD photometry data base in V and I band is needed to take advantage of it.

ACKNOWLEDGEMENTS: This paper is supported by Creative Research Initiatives of the Korean Ministry of Science and Technology.

REFERENCES

Carretta, E., & Bragaglia, A. 1998, A&A, 329, 937
Carretta, E., & Gratton, R. G. 1997, A&A, 121, 95

Chaboyer, B., Demarque, P., Kernan, P. J., & Krauss, L. M. 1998, ApJ, 494, 96
Clement, C. M. 1999, private communication
Da Costa, G. S., & Armandroff, T. E. 1990, AJ, 100, 162
Fusi Pecci, F., Ferraro, F. R., Crocker, D. A., Rood, R. T., & Buonanno, R. 1990, A&A, 238, 95
Iben, I. 1968, Nature, 220, 143
Johnsohn, J. A., & Bolte, M. 1998, AJ, 115, 693
Kraft, R. P., Sneden, C., Langer, G. E., & Prosser, C. F. 1992, AJ, 104, 645
Kurucz, R. L. 1992, in IAU Symp. 149, The Stellar Populations of Galaxies, ed. B. Barbuy & A. Renzini (Dordrecht: Kluwer), 225
Landolt, A. U. 1992, AJ, 104, 340
Rood, R. T., Carretta, E., Paltrinieri, B., Ferraro, F. R., Fusi Pecci, F., Dorman, B., Chieffi, A., Straniero, O., & Buonanno, R. 1999, ApJ, 523, 752
Sarajedini, A. 1994, AJ, 107, 618
Sarajedini, A., & Forrester, W. L. 1995, AJ, 109, 1112
Sawyer-Hogg, H. 1973, A 3rd Catalogue of Variable Stars in Globular Clusters
Sneden, C., Kraft, R. P., Prosser, C. F., & Langer, G. E. 1992, AJ, 104, 2121
Stetson, P. B. 1987, PASP, 99, 191
Stetson, P. B. 1990, PASP, 102, 932
Stetson, P. B. 1992, in IAU Colloq. 136, Stellar PhotometryCurrent Techniques and Future Developments, ed. C. J. Butler & I. Elliot (Cambridge: Cambridge Univ. Press), 291
Stetson, P. B., & Harris, W. E. 1988, AJ, 96, 909
Zinn, R., & West, M. J. 1984, ApJS, 55, 45